IUBAT Review
A Multidisciplinary Academic Journal

Md. Jubaer Alam, Firuz Ahamed Nahid, Md. Turiqul Islam, 2019. "**Design of a Broad Band – Stop Filter with Metamaterial as Defective Ground System**" *IUBAT Review* 2 (1): 41-48. iubat.edu/journal

Design of a Broad Band – Stop Filter with Metamaterial as Defective Ground System

Md. Jubaer Alam [1*], Firuz Ahamed Nahid [1], Md. Turiqul Islam [1].

[1]Department of EEE, IUBAT-International University of Business Agriculture and Technology, Dhaka, Bangladesh

*Corresponding author: E-mail: jubaer.alam@iubat.edu

ABSTRACT: *In this article, a defected ground structure (DGS) is introduced to design a broad band-stop filter to adjust the resonating characteristics by varying the dimension of the structure. The proposed antenna is embedded into a 50Ω microstrip framework. FR-4 (Lossy) is used as a substrate to design the proposed broad band-stop filter which has a succinct structure. The attainment of the antenna is explored both integrally and experimentally. Here Complementary Split Ring Resonator (CSRR) is introduced in the ground layer. It has been monitored that the level of rejection of the filter in the stopband region keeps on going with the introduction of CSRR. This filter is advisable for X-band applications especially on 5.9 to 11.3GHz. The Nicolson-Ross-Weir approach has been applied at the filtering frequency. The effective electromagnetic parameters retrieved from the simulation of the S-parameters imply that metamaterial antenna shows negative refraction bands. This indicates that the proposed antenna has behavior to justify the obligation as a Left Handed medium.*

KEYWORDS: Band-stop filter, Defected ground plane, Left-handed medium Band-stop filter, Defected ground plane, Left-handed medium.

1. Introduction

After getting the commercial authorization from the Federal Communication Commission (FCC) in February 2002, Ultra-wideband (UWB) applications had become very popular at home and abroad (Yin *et al.,* 2008). But this UWB system has to go through probable interferences for WiMax, WLAN and RFID. Thus the use of RF components that operate in multiple bands has become important to handle this complexity. A lot of researches has been made on the development of filter technology. In today's world, one of the most essential parameters is confinement among channels in a particular bandwidth. Despite avoiding possible interferences in a system, Band-stop filter (BSF) is one of the competent arrangements to notify this problem by combining them with the system. In progression, a lot of researches has been done to flourish different kinds of BSF (Jiang *et al.,* 2016).

From the last few years, transmission lines have been used with patterned ground structures like spaces, gaps, and slots, which has shown interesting characteristics inclusive of band-stop and slow-wave phenomena (Radisic *et al.,* 1998; Ahn *et al.,* 2001; Caloz *et al.,* 2004). These specially arranged structures are commonly known as slotted ground structure or defected ground structure (DGS) (Caloz *et al.,* 2004). Park et al. in 1991 proposed this DGS for its improved quality of filter behaviors and reduction of filter size (Kim *et al.,* 2000). Moreover, this DGS has good command over the performance enhancement of stop-band filters, suppression of good harmonics, and distinguished periodic system (Xiaol and Fu 2010). DGS quenches the response of the effective inductance and capacitance of a microstrip line only by changing the size and shape of it. As a result, the execution of the filter and its circuit can be enhanced. The performance of the filter turned to a different level when metamaterials were introduced.

Metamaterials are the special type of materials that are usually not available in nature. They are engineered materials, and they need embedding periodic unit cells for their formation to create naturally unavailable electromagnetic properties. Moreover, these materials have the power to control the electromagnetic wave beams to show their unorthodox characteristics. These unusual features of the metamaterials depend on the geometry of the atomic construction. It has been started from the year 1968, Veselago et al observed unique properties of materials having negative permittivity (ε) and permeability (μ). But it was not appreciated until 2000 when Smith et al. fortunately validated a new unreal with these unconventional properties (both permittivity and permeability were negative) is called left-handed metamaterial. In the case of negativity, it has been categorized as Single-negative (either permittivity is negative or permeability is negative), Double-negative (both permittivity and permeability are negative). There is also a term called near-zero refractive index metamaterial (NZRI) where the permittivity and permeability of material become approximately zero of a particular range of frequency. Having these captivating electromagnetic phenomena, necessary applications, like SAR reduction (Faruque *et al.,* 2012), superlenses, antenna design (Islam *et al.,* 2015), filters (Fang *et al.,* 2014; Naib *et al.,* 2013), invisibility cloaking (Landy *et al.,* 2013), electromagnetic absorber, and electromagnetic band gaps, etc can be employed by metamaterials.

Resonant type metamaterials are used in filter applications. A variety of subwavelength resonators are used, such as split-ring resonators

(SRRs), complementary split-ring resonators (CSRRs), double Slit split-rings resonators (DS-SRRs), double Slit complementary split-rings resonators (DS-CSRRs) (Jindal *et al.,*

2012), etc.

In this paper, a fusion is made by a complementary split-ring resonator (CSRR) in the ground plane as a defected ground system so that the structure can mostly work in the X-band region as a broad band-stop band filter.

2. Depiction and configuration

Fig. 1 shows the proposed band-stop filter. The resonating frequency confides on the physical aspects of the structure. The concentration of the structure can be realized depending on the specifications derived from the equivalent circuit Fig. 1 (c) proposed by Woo et al. (Woo *et al.,* 2006). On the other hand, the cut off frequency of this type of filter can be accustomed by maintaining suitable values of the elements of the filter. However, to

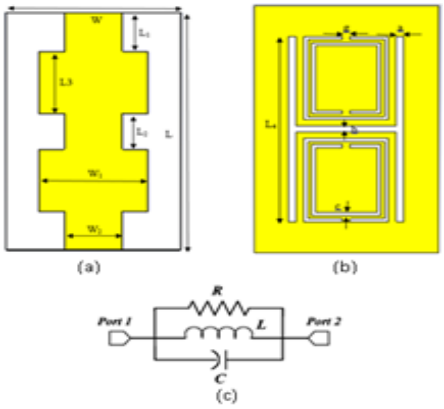

Figure 1: Geometry of the proposed broad band-stop filter (a) front view; (b) back view and (c) equivalent ckt model of the band stop resonator

understand the expected values of lumped filter elements, it is essential to determine the aspects of these transmission lines. The proposed filter is contrived and constructed on a composite material named as glass-reinforced epoxy laminate or FR-4 substrate. This substrate has a height of 1.60 mm and a relative dielectric constant (εr) of 4.4 and loss tangent tan δ=0.02. Defected Ground Structure (DGS) has a direct connection with the photonic bandgap (PBG). It can be extracted directly from PBG and can be realized when this defected structure is depicted on the ground. This defectiveness in the ground plane interrupts the shield current. This may cause an increment of effective capacitance and inductance in the transmission line (Radisic *et al.,* 1998). CSRRs are used as DGS under the modified microstrip line. Even resonant frequency can be controlled if the microstrip line and the DGS are modified.

Table 1: Parameters of the unit cell

Parameters	**L**	**L_1**	**L_2**	**L_3**	**L_4**	**W**
Dimensions (mm)	40	6.5	6	10.5	27	24
Parameters	W1	W2	a	b	c	g
Dimensions (mm)	**15**	**8**	**1**	**1**	**0.5**	**0.5**

This DGS influences in implementing compact capacitive coupling to the line are called microstrip DGS. The cutoff frequency of the filter depends on the overall slot size. This cut off frequency can be adjusted by varying the slot size. It is essential to reduce the inductance of the stripline if the resonant frequency needs to be shifted up instead of back, or widening the stripline may help to reduce the inductance of the filter. Table 1 shows the parameters of the filter. Commercially available Finite Integration

Technique (FIT)-based on Computer Simulation Technology (CST) Microwave Studio software was used to simulate the proposed filter.

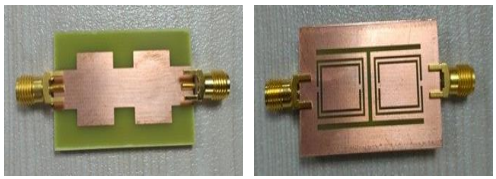

(a) (b)

Figure 2: Prototype of the Band stop filter (a) Front view and (b) Back view

3. Results and Discussions

The filter is designed on FR-4 (substrate) with an area of 24×40 mm2. A parametric study is made on the dimension of the filter to justify the insertion loss. CSRR in the ground plane is used and the results are compared with the conventional one. There are plenty of ways to find out the effective parameters of a unit cell-like Nicolson-Ross-Weir (NRW) method, direct retrieval method of refractive index (DRI), etc. This paper highlights the electromagnetic properties using the real values of ε, μ, and η using S11 and S21.

Fig. 3 shows the parametric study of the filter and a decision is made on return/insertion loss characteristics. The simulation is made on 5 to 15 GHz that justifies its unorthodox pattern. In the microstrip line, the width places the main role to adjust the inductive effect. A decrease in inductance shifts the resonant to higher frequencies.

Fig. 3 (a) exhibits the return loss of the structure with various shapes of the microstrip line. Keeping the ground unchanged, the microstrip line has been made three different structures. The microstrip line with modification shows a

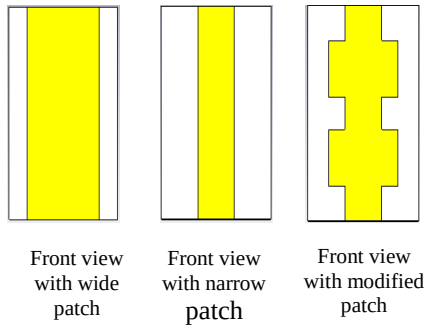

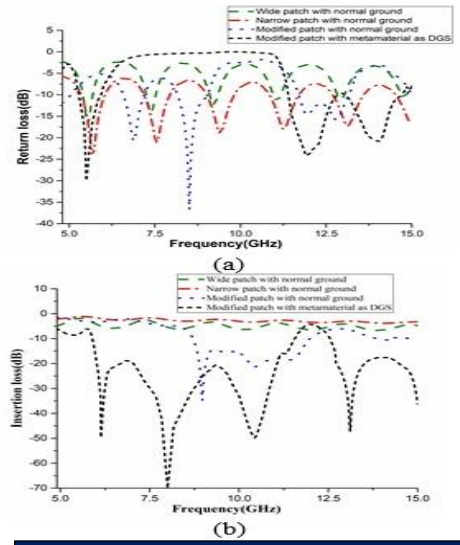

Fig. 3 Simulated return/ insertion loss characteristics for different structures (a) return loss & (b) insertion

less fluctuating response than the other two. But with the use of DGS, the return loss reaches near-zero line or less than -10dB line in the frequency range of 5.9 to 11.3 GHz. The application of CSRR has made the bandgap in this frequency range.

Fig. 3 (b) exhibits the insertion loss of the configuration with the same three different microstrip lines. Firstly, the loss is observed by applying normal ground and lately, DGS is applied. The modified microstrip line shows a better bandgap than the other two, so DGS is applied on the ground of the modified microstrip. The insertion loss curves cross the -10dB line at 5.3GHz and come back to zero lines at 11.3GHz. The influence of CSRR in the ground plane makes the insertion loss wider.

Fig. 4 shows the flat response of return and insertion losses at about 5.9 to 11.9 GHz. Comparatively a wider stop-band has acquired. Moreover, the proposed structure shows broader and deeper band coverage than traditional stop-band filters (Ojaroudi *et al.*, 2012; Pourbagher *et al.*, 2015). There is a bit divergence between simulated and measured values. This difference is predominantly due to a few parameters like fabrication, dielectric constant, and thickness of the substrate, large simulation frequencies, and the effect of SMA (Faraghi *et al.*, 2014; Pourbagher *et al.*, 2017). It is better to check the manufacturing and the measurement process to get a good deal of return loss characteristics for the structure. However, soldering accuracy of the SMA, quality of the substrate, and no rusting in the structure need to be considered.

3.1. Analysis of Effective parameters

The series of gaps affect the structure for its negative effective permeability. Combining these CSRRs and gaps create a narrow bandgap

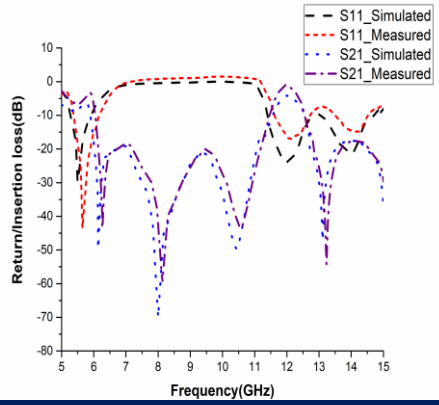

Fig. 4: Simulated and measured return/ insertion loss for the proposed band stop filter

continuously permeability and permittivity emerged close to the resonant frequency (Fang *et al.*, 2014).

To differentiate the effective permittivity (ε_r) and permeability (μr) with S11 and S21, the Nicolson-Ross-Weir (NRW) method is applied.

$$\varepsilon_r = \frac{c}{j\pi fd} \times \frac{(1-v_1)}{(1+v_1)} \qquad (1)$$

$$\mu_r = \frac{c}{j\pi fd} \times \frac{(1-v_2)}{(1+v_2)} \qquad (2)$$

The effective refractive index (η_r) can also be calculated from and (Jiang *et al.*, 2016):

$$\eta_r = \frac{c}{j\pi fd} \times \sqrt{\frac{(S_{21}-1)^2 - S_{11}^{\ 2}}{(S_{21}+1)^2 - S_{11}^{\ 2}}} \qquad (3)$$

Fig. 5(a) shows negative permittivity at resonating points. It shows negativity at 5.49 to 5.81GHz, 6.12 to 6.44GHz, 7025 to 8.01GHz, 8.97 to 10.97GHz, 11.17 to 12.02GHz and 12.86 to 14.08GHz. Fig.5 (b) shows the negative permeability at 5 to 6.11GHz, 6.56 to 7.31GHz, 7.97 to 8.29GHz, 8.84 to 9.44GHz, 11.34 to 11.47GHz, 12.34 to 12.75GHz and 13.80 to

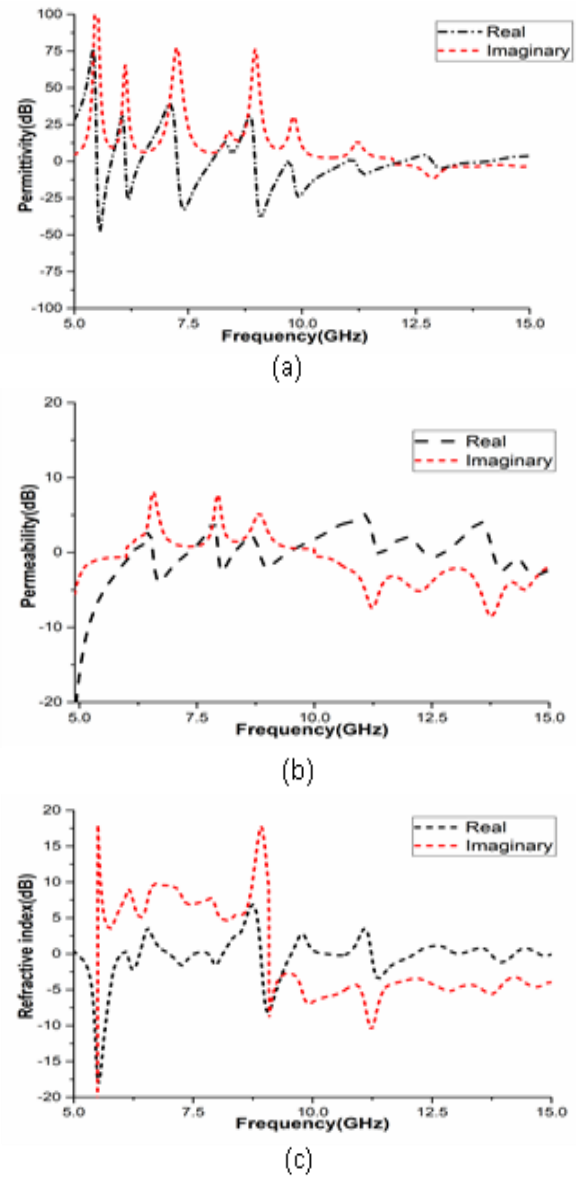

Fig. 5 (a) Effective permittivity (ε) vs frequency; (b) effective permeability (μ) vs frequency; (c) refractive index (η) vs frequency

15GHz. At lower frequencies, the current flow matches the applied field. But in case of higher frequencies, the current can't make a go of it with the applied field when the permeability becomes negative. In the gap, there is a charge produced of a CSRR, which is regulated to a fluctuating magnetic field. At low frequency, the current remains in phase with the applied field, but it fails to remain in phase in higher frequencies and as a result, negative permeability produces.

In Fig. 5(c), real and imaginary parts of η are plotted as a function of frequency. The curve shows negativity at 5.05 to 6.00GHz, 6.11 to 6.38GHz, 7 to 7.52GHz, 7.82 to 8.11GHz, 8.93 to 9.54GHz, 10.25 to 10.73GHz, 11.23 to 12.14GHz, 13.73 to 14.22GHz and 14.74 to 15 GHz.

Table 2 shows the frequency range of refractive indices with effective parameters of the filter at different frequency bands. The refractive index shows negativity when the permittivity and permeability both become negative. Here η shows certain negativity at different bands of frequencies. Hence, the designed filter has significant portions where all the three effective parameters become negative. Therefore, this band-stop filter can be claimed as double-negative metamaterial as it has negative peaks at 5.51, 7.29, 7.97, 9.05, 11.37, and 13.93GHz in all the three effective parameters which are shown in Table 2 with bandwidths.

Table 2: Parameters of the unit cell		
Effective parameters	Frequency Range(GHz)	Covered Bands
Permittivity (ε)	5.49 to 5.81, 6.12 to 6.44, 7025 to 8.01, 8.97 to 10.97, 11.17 to 12.02 & 12.86 to 14.08GHz.	C, X & Ku
Permeability (μ)	5 to 6.11, 6.56 to 7.31, 7.97 to 8.29, 8.84 to 9.44, 11.34 to 11.47, 12.34 to 12.75 & 13.80 to 15GHz.	C, X & Ku
Refractive Index (η)	5.05 to 6.00, 6.11 to 6.38, 7 to 7.52, 7.82 to 8.11, 8.93 to 9.54, 10.25 to 10.73, 11.23 to 12.14, 13.73 to 14.22GHz & 14.74 to 15 GHz.	C, X & Ku

4. Conclusions

This paper presents the framework of the broad bandstop filter using a modified microstrip line and defected ground structure. Implementation of CSRR in the ground plane creates a constant and flat impedance bandwidth of almost 5.4GHz (5.9 to 11.3 GHz). To justify the performance of the proposed filter an analogy is conferred on transmission coefficient, relative permeability, permittivity, and refractive index. The effective parameters of the filter cover C, X, and Ku-band independently with double negative phenomena at C, X, and Ku-band. Due to its auspicious design, double-negative characteristics and the proposed structure have the potential to be used as Broad band stop filter

References

Ahn, D., J. Park, A. Member, C. Kim, S. Member, J. Kim, S. Member, Y. Qian, T. Itoh, and L. Fellow 2001. A Design of the Low-Pass Filter Using the Novel Microstrip Defected Ground Structure, IEEE Trans. Micr. Theory and Tech., 49, 1: 86–93.

Al-Naib, I., Jansen, C., Singh, R., M. Walther and M. Koch 2013. Novel THz metamaterial designs: From near- and far-field coupling to high-q resonances, IEEE Trans. Terahertz Sci. Technol. 3: 772–782.

Caloz, C., H. Okabe, T. Iwai, and T. Itoh 2004. A Simple and Accurate Model for Microstrip Structures with Slotted Ground Plane, IEEE Micr. And Wire. Comp. Lett. 14, 4: 133–135.

Fang, C.Y., J.S. Gao and H. Liu 2014. A novel metamaterial filter with stable passband performance based on frequency selective surface, AIP Adv. 4: 077114.

Faraghi, A., M. Ojaroudi and N. Ghadimi 2014. Compact microstrip low-pass fikter with sharp selection characteristics using triple novel defected structures for UWB applications, Micro. And Opt. Tech. Lett. 56, 4: 1007-1010.

Faruque, M.R.I., M.T. Islam and N. Misran, Design analysis of new metamaterial for EM absorption reduction 2012. Prog. Electromagn. Res. 124: 119–135.

Islam, M. M., Islam, M.T., M. Samsuzzaman and M.R.I. Faruque 2015. Compact metamaterial antenna for UWB applications, Electron. Lett. 51: 1222–1224.

J. Xiaol and Y. Z. J. S. Fu 2010. Non-uniform DGS Low Pass Filter with Ultra-wide Stopband, IEEE, 1216–1219.

Jiang, T., Y. Wang, and Y. Li 2016. Design, and Analysis of a Triple Stop-band Filter Using Ratioed Periodical Defected Microstrip Structure, De Gruyter, 71: 1-7.

Kim, C., Member, S., Park, J., Member, A., D. Ahn, and J. Lim 2000. A Novel 1-D Periodic Defected Ground Structure for Planar Circuits, IEEE Micr. And Guid. Wave Lett. 10, 4: 131–133.

N. Landy and D.R. Smith 2013. A full-parameter unidirectional metamaterial cloak for microwaves, Nat. Mater. 12: 25–28.

Ojaroudi, M., Ojaroudi, N., R. Habibi and H. Ebrahimian 2012. Microstrip low-pass fikters by using novel defected ground slot with a pair of protruded t-shaped strips inside the slot, Adv. Elec. Symp, AES 2012, Paris, France, Apr. 16-19.

Pourbagher, M., J. Nourinia and C. Ghobadi 2017. Compact Broad Band-Stop Filter with Circular Fractal-Shaped Stubs for X-Band Radar Applications, App. Comp. Elec. Society (ACES) Journal,32, 1: 56-59.

Pourbagher, M., Ojaroudi, N., J. Nourinia and C. Ghobadi 2015. Compact band-stop filter for X-band transceiver in radar applications, App. Comp. Elec. Society (ACES) Journal, 30, 4: 423-428.

Radisic, V., S. Member, and Y. Qian 1998. Novel 2-D Photonic Bandgap Structure for Microstrip Lines, IEEE Micr. And Guid. Wave Lett. 8, 2: 69–71.

S. Jindal 2012. Review of Metamaterials in Microstrip Technology for Filter Applications, Intl. Jour. Comp. App. 54, 3: 48–54.

Woo, D., Lee, T., Lee, J., C. Pyo, and W. Choi 2006. Novel U-Slot and V-Slot DGSs for Bandstop, IEEE Trans. Micr. Theory and Tech. 54, 6: 2840–2847, 2006.

Yin, X., Ruan, C., Mo, S., Ding, C., and J. Chu 2008. A Compact Ultra-Wideband Microstrip Antenna with Multiple Notches, Prog. Electromagn. Res., 84: 321–332.